# Expression of a p16$^{INK4a}$-specific ribozyme downmodulates p16$^{INK4a}$ abundance and accelerates cell proliferation

Jesper Nylandsted[a,*], Mikkel Rohde[a], Jiri Bartek[a], Michael Strauss[a,b]

[a] *Danish Cancer Society, Institute of Cancer Biology, Strandboulevarden 49, DK-2100 Copenhagen Ø, Denmark*
[b] *Humboldt University, Max Delbrück Center for Molecular Medicine, D-13122 Berlin-Buch, Germany*

Received 15 August 1998

**Abstract The p16$^{INK4a}$ tumor suppressor negatively regulates progression through the G1 phase of the mammalian cell cycle. To mimic the downmodulation of p16$^{INK4a}$ commonly seen in cancer, we designed and characterized a hammerhead ribozyme against exon E1α of the murine p16$^{INK4a}$ transcript. Stable expression of the ribozyme in murine erythroleukemia (MEL) cells reduced the endogenous p16$^{INK4a}$ protein by more than 70% and significantly accelerated cell cycle progression. The specificity and efficiency of our new ribozyme suggest its possible application in elucidating the role of p16$^{INK4a}$ in fundamental biological processes including homeostatic tissue renewal, protection against oncogenic transformation, and cellular senescence.**



*Key words:* p16$^{INK4a}$ tumor suppressor; Hammerhead ribozyme; Cell cycle; MEL cell

## 1. Introduction

Progression through the mammalian cell division cycle is controlled by periodic activation of the cyclin-dependent kinases (Cdks) [1,2]. The Cdks are activated by association with their regulatory partners, the cyclins, whose expression oscillates throughout the cell division cycle [1]. In mid-to-late G1 phase of the cell cycle Cdk4 and Cdk6 assemble with D-type cyclins and phosphorylate their major substrate, the retinoblastoma protein (pRb) [2,3]. In its hypophosphorylated state, pRb binds diverse transcription factors including E2F and acts as a negative cell cycle regulator by preventing S-phase entry. The phosphorylation of pRb in late G1 releases E2F which in turn triggers expression of genes essential for S-phase entry and progression through the cell cycle [3,4].

The p16$^{INK4a}$ tumor suppressor protein negatively regulates the progression of cells through the G1 phase of the cell cycle by inhibiting the functions of Cdk4 and Cdk6 [5,6]. Loss of functional p16$^{INK4a}$ results in upregulated Cdk4/Cdk6 kinase activity, leading to persistent pRb hyperphosphorylation and thereby contributes to deregulation of cellular proliferation. The involvement of p16$^{INK4a}$ in carcinogenesis was established by observations that the INK4a locus is mutated, deleted, or silenced by promoter methylation in a number of human cancer types [2,7,8].

The INK4a locus has the unusual capacity to generate two transcripts derived from different promoters. Each transcript has a unique 5′ exon, E1α and E1β, each of which is joined to exon 2 and 3 through a common splice acceptor site in exon 2. The α and β transcripts encode two different proteins. The α transcript encodes p16$^{INK4a}$, whereas the β transcript encodes the p19$^{ARF}$ protein from an alternative reading frame initiated within the E1β exon [9–11].

Here we have designed ribozymes targeted to the p16$^{INK4a}$ α transcript in order to provide a specific tool to downmodulate the expression of p16$^{INK4a}$ as an approach to study its function. The potential of using *trans*-acting ribozymes to study the function of a particular gene is underscored by their attractive features as catalysts: they have the capacity of cleaving RNA, and potentially inactivate multiple copies of a target RNA [12]. Furthermore, ribozymes might be more effective than antisense strands even under non-turnover conditions because their activity cleaves the target, thereby eliminating the possibility that subsequent denaturation of the complex could reactivate the target RNA [13].

Despite recent progress, the development of effective ribozymes for in vivo applications is still difficult and strongly depends on the rational design of the ribozyme. There are several aspects important for the successful application, including ribozyme kinetics, its stability, target site accessibility, expression strategy and ribozyme-target colocalization [14,15].

The utilization of ribozyme expression cassettes as carriers for ribozymes was shown to fulfil several criteria for in vivo applications. Expression units based on naturally occurring RNAs like tRNA [16] or Va I RNA derived from adenovirus [14,17,18] allow for high-level polymerase III expression and a stable structure of the ribozyme. These expression strategies furthermore deliver the ribozyme to the cytoplasm and should colocalize it with the target RNA [19].

In this paper, we have used an optimized ribozyme expression cassette based on the Va I gene derived from adenovirus type 2 [14]. We show that the ribozyme embedded in the expression cassette can cleave both in vitro and in vivo and is able to downmodulate the p16$^{INK4a}$ protein level by at least 70% when expressed in mouse erythroleukemia (MEL) cells. Furthermore, MEL clones expressing the ribozyme construct gained a significant proliferative advantage.

## 2. Materials and methods

### 2.1. Plasmid constructs

The murine p16$^{INK4a}$ full-length cDNA construct was made by combining two cDNA clones: one containing the untranslated 5′ region and coding region (kindly provided by Manuel Serrano, Cold Spring Harbor) and another clone with the coding sequence and the 3′ untranslated region (kindly given by Dawn Quelle, St. Jude Research Hospital). The 5′ clone was PCR amplified and subcloned into the pCRII (Invitrogen) vector and the 3′ clone was inserted into the *Kpn*I/*Bsp*1191 sites generating the full-length mouse cDNA clone pCRII-p16$^{INK4a}$.

The ribozyme constructs were made by fusing oligonucleotides (DNA Technology) representing each strand. The ribozyme sequences containing *Xho*I/*Nsi*I sites were cloned into the *Sal*I/*Pst*I sites in the

*Corresponding author. Fax: +45 (3525) 7721.
E-mail: jnl@biobase.dk


PII: S0014-5793(98)01089-8

GVal plasmid as according to [14]. The sequences of the ribozyme oligonucleotides were: Rz 89-12: 5′-CGAGCAGCGCTGATGAGTCCGTGAGGACGAAACTCCAATGCA-3′ and 5′-TTGGAGTTTCGTCCTCACGGACTCATCAGCGCTGC-3′; Rz 89-15: 5′-TCGAGTGCAGCGCTGATGAGTCCGTGAGGACGAAACTCCATGATGCA-3′ and 5′-TCATGGAGTTTAGTCCTCACGGACTCATCAGCGCTGCAC-3′.

The Va expression cassette containing Rz 89-12 was excised using *Xba*I and *Hin*dIII and cloned into the *Spe*I-*Hin*dIII sites in the cytomegalovirus (CMV) promoter plasmid, pX [20].

### 2.2. In vitro transcription

In vitro transcription was performed by incubating 2 μg of linearized template (*Hin*dIII linearized pCRII-p16$^{INK4a}$ or *Nhe*I linearized GVal vector) in RNA polymerase buffer with 25 units of T7 RNA polymerase (Biolabs) for 1 h at 37°C according to manufacturers specifications. In the p16$^{INK4a}$ transcription reaction, 2 mM GTP, ATP, UTP and 1 mM CTP plus 5 μCi of [$^{32}$P]-CTP was included.

### 2.3. Ribozyme cleavage in vitro

In vitro cleavage was done by incubating different molar ratios of labeled p16$^{INK4a}$ RNA and ribozyme RNA in 50 mM Tris-HCl (pH 7.5). The reactions were incubated at 95°C for 90 s and subsequently cooled on ice. $MgCl_2$ was added (or excluded) to a final concentration of 10 mM and the 20 μl reactions were incubated at 37°C for 1 h. Ten μl of stop buffer (95% formamide, 20 mM EDTA, 0.05% bromphenol blue, 0.05% xylene cyanol) was added and the reactions were loaded on a 5% denaturing polyacrylamide gel and run in Tris-Borate buffer. The gels were exposed on a phosphorimager screen.

### 2.4. TNT coupled transcription/translation assay

130 ng of *Hin*dIII linearized pCRII-p16$^{INK4a}$ or pCMV human p16$^{INK4a}$ plasmid was incubated with 1 μg or 2 μg of *Hin*dIII linearized plasmids of ribozymes or GVal vector (plasmid ratio 1:5 or 1:10). The plasmid DNA was mixed with TNT rabbit reticulocyte lysate (Promega), reaction buffer, amino acid mix (-met), 35S-methionine, RNasin and T7 RNA polymerase and incubated at 30°C for 1.5 h according to manufacturers instructions. 1/5 of each reaction mixture were analyzed by 15% SDS-PAGE.

### 2.5. Tissue culture and transfections

MEL cells, DS19/Sc9 derived from 745A cells [21] were maintained in α-minimal essential medium (Sigma) supplemented with 10% fetal calf serum (Gibco Brl) at 37°C in a humidified 5% $CO_2$ atmosphere. Establishment of stable transfected clones was performed by the pX-ribozyme construct with a neomycin gene containing plasmid (pCMV-Neo) in the molar ratio of 10:1 using electroporation (settings: 300 V; 250 μFD; ∞ Ω). Cells were cultured in medium supplemented with 1 mg/ml G-418 sulphate (Life Technologies) and resistant clones were isolated after 12 days. Clones were screened for ribozyme expression by RT-PCR using primers specific for the Va I-Va II genes.

### 2.6. Northern blotting

Total RNA from MEL cells was purified using the guanidinium thiocyanate method as described [22]. Ten μg of total RNA from each clone was separated on denaturing formaldehyde gel and blotted onto Hybond-N nylon membrane (Amersham) using capillary transfer. The probes were generated using the random primed labeling kit (Boehringer Mannheim) by incorporation of [α$^{32}$P]-dCTP. A full-length p16$^{INK4a}$ DNA fragment was labeled and used as the probe. The blots were exposed on a phosphorimager screen.

### 2.7. Immunoblotting

Cells were harvested, frozen in liquid nitrogen and proteins extracted in buffer containing 50 mM HEPES (pH 7.5), 250 mM NaCl, 5 mM EDTA, 0.1% NP-40, 1 mM DTT (Protease inhibitors: leupeptin 2.5 μg/ml, aprotinin 2 μg/ml, PMSF 50 μg/ml). Western blotting was performed according to standard procedures using Bio-Rad minigel apparatus, semidry blotting equipment (Millipore) and nitrocellulose membranes (MFS). Protein bands were visualized by enhanced chemiluminescence (Amersham). For detection of p16$^{INK4a}$ protein, a rabbit polyclonal antibody against mouse p16$^{INK4a}$ was used (Santa Cruz Biotechnology). Cdk4 protein was detected by an antibody (DCS 31) recognizing an epitope corresponding to amino acids 15–25 of Cdk4 (our unpublished results).

## 3. Results

### 3.1. Cleavage of mp16$^{INK4a}$ mRNA in vitro by a transcribed ribozyme

Accessible ribozyme cleavage sites within mouse p16$^{INK4a}$ RNA were chosen on the basis of a computer assisted prediction of the RNA secondary structure (RNAFOLD program, Wisconsin package). Only those potential cleavage sites predicted to be in single-stranded loop structures were considered. The GUC site at nucleotide (nt) 89 positioned just after the start codon in exon E1α [23] was chosen and ribozyme genes were designed against this cleavage site. The length of the complementary ribozyme recognition sequences (helices I and III) were either 15 nt (Rz 89-15) or 12 nt (Rz 89-12) (Fig. 1A). The shorter flanking nt in Rz 89-12 might facilitate a faster dissociation of the ribozyme from the cleaved substrate and allow further ribozyme turnover reactions to occur.

In order to obtain ribozymes for in vivo applications, the

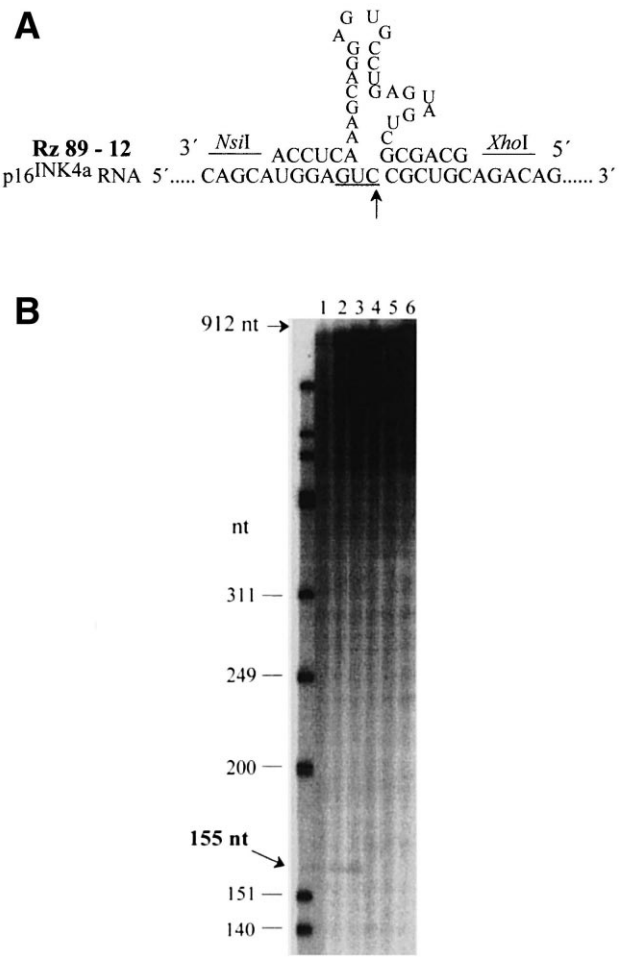


Fig. 1. Properties of the ribozyme (A) nucleotide sequence of Rz 89-12. The cleavage site at nt 89 in the p16$^{INK4a}$ transcript is indicated (arrow). B: In vitro cleavage analysis of the ribozyme Va expression unit. Ribozyme RNA and labeled p16$^{INK4a}$ RNA substrate were combined in 10 mM $MgCl_2$, heat denatured and incubated at 37°C for 1 h. The samples were run on a 5% denaturing polyacrylamide gel with a [$^{32}$P]-labeled DNA marker. Lanes 1–3: Rz 89-12 and p16$^{INK4a}$ in the molar ratios 10:1, 20:1 and 50:1. Lanes 4–5: Va RNA (minus ribozyme) and p16$^{INK4a}$ in the ratios 20:1 and 50:1 (negative control). Lane 6: Rz 89-12 and p16$^{INK4a}$ in the ratio 50:1 without $MgCl_2$. The full-length p16$^{INK4a}$ transcript (912 nt) and the 155 nt cleavage fragment are indicated by arrows.

ribozymes were cloned into an adenovirus Va RNA expression cassette. The cassette contains a chimerical stem-loop sequence allowing the catalytic sequences to be formed independently from surrounding RNA structures [14]. To asses the ability of the designed ribozymes embedded in Va expression cassettes to cleave in vitro, RNAs were synthesized and incubated with radiolabeled substrate RNA. The 912 nucleotide substrate RNA (846 nucleotides of $p16^{INK4a}$ plus 66 nt of vector sequence) was prepared by in vitro transcription. In each reaction, 100 nM of labeled $p16^{INK4a}$ RNA were incubated with ribozyme RNA in different molar ratios (Fig. 1B). Similar cleavage activities were observed for Rz 89-15 (not shown) and Rz 89-12 and cleavage generated the expected small 5′ fragment of 155 nucleotides (89 nucleotides of $p16^{INK4a}$ plus 66 nt derived from the vector sequence). The larger cleavage fragment (757 nt) generated was not recognizable because of dominant heterogeneous transcripts arisen during the in vitro transcription of $p16^{INK4a}$ cDNA. No cleavage was detected in the absence of $MgCl_2$ due to the requirement for divalent metal ions in cleavage catalysis (Fig. 1B, lane 6).

### 3.2. Inhibition of in vitro translation by ribozymes specific for murine $p16^{INK4a}$

To further analyze and confirm the ribozyme specificity for $p16^{INK4a}$ in vitro, a coupled TNT transcription/translation system (Promega) was used. The standard assay was used to detect the ability of the ribozymes to downmodulate $p16^{INK4a}$ measured on the protein level. 130 ng of substrate $p16^{INK4a}$ plasmid (pCRII-$p16^{INK4a}$) was combined with ribozyme plasmids or with Gval plasmid (Va cassette minus ribozyme) in different molar ratios and incubated at 30°C for 1.5 h (Fig. 2). Rz 89-15 and Rz 89-12 reduced the level of $p16^{INK4a}$ considerably. At a molar ratio of 10:1 (ribozyme:substrate), the level of $p16^{INK4a}$ was reduced by more than 95% (Fig. 2A, lanes 5 and 6). Both ribozymes seemed to reduce the $p16^{INK4a}$ level with similar efficiency. To examen whether the ribozyme activity observed was specific for murine $p16^{INK4a}$, the ribozymes were incubated with human $p16^{INK4a}$. No inhibition was detected in this case (Fig. 2B).

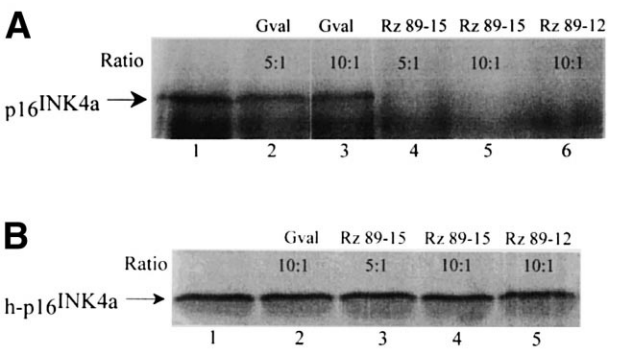


Fig. 2. Ribozyme activity assay. In vitro coupled transcription/translation of $p16^{INK4a}$ plasmid was performed and the 35S methionine labeled proteins separated by SDS-PAGE on 15% gels. A: Lane 1: $p16^{INK4a}$ alone. Lanes 2 and 3: Gval vector and $p16^{INK4a}$ in the molar ratios 5:1 and 10:1 (control). Lanes 4–6: plasmids of Rz 89-15 and Rz 89-12 incubated with $p16^{INK4a}$ in the ratios 5:1, 10:1 and 10:1. B: The two ribozyme plasmids and a human $p16^{INK4a}$ plasmid.

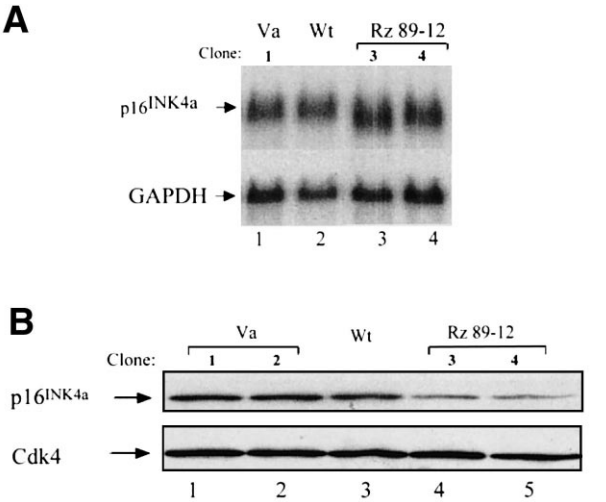


Fig. 3. In vivo analysis of ribozyme function. A: Northern blot analysis of $p16^{INK4a}$ expression of clones stably transfected with the ribozyme construct. The membrane was probed with a $p16^{INK4a}$ fragment (900 nt) (upper panel). Lane 1: clone transfected with the control Va plasmid. Lane 2: wild-type (Wt) cells. Lanes 3–4: two clones expressing the Rz 89-12 construct. The lower panel shows glyceraldehyde 3-phosphate dehydrogenase (GAPDH) expression as control for equal loading. B: Immunoblotting analysis of the $p16^{INK4a}$ protein (18 kDa) levels (upper panel). Lanes 1–2: two Va plasmid transfected clones. Lane 3: wild-type cells. Lanes 4–5: the two clones expressing Rz 89-12. Cdk4 (32 kDa) was used as internal control for equal loading (lower panel).

### 3.3. Function of the stably expressed ribozyme in vivo

In order to study the cleavage efficiency of the ribozyme on $p16^{INK4a}$ mRNA in vivo, Rz 89-12 was subcloned into a mammalian expression vector containing the CMV promoter and a polyadenylation signal. A murine erythroleukemia cell line (MEL), known to express a functional pRb [21] and elevated $p16^{INK4a}$ [23] was chosen as a cellular test system to analyze the in vivo function of Rz 89-12. Stably transfected clones were established and two ribozyme expressing clones were identified by RT-PCR and further analyzed on the RNA level by Northern blotting (Fig. 3A). As expected, the level of $p16^{INK4a}$ mRNA was not reduced in the ribozyme expressing clones. However, a fraction of the RNA migrates faster and most likely represents the 757 nt cleavage product generated by cleaving of 89 nt (Fig. 3A, lanes 3–4). The protein level of $p16^{INK4a}$ was determined for the different clones by immunoblotting. The two clones expressing Rz 89-12 had significantly reduced $p16^{INK4a}$ protein levels (Fig. 3B, lanes 4–5). The reduction was estimated to be 73% when compared to the Va control clones and wild-type cells (Fig. 3B, lanes 1–3). These results indicate that Rz 89-12 is able to down-regulate the level of $p16^{INK4a}$ in MEL cells.

### 3.4. Enhanced proliferation of ribozyme expressing MEL clones

Growth experiments were performed with ribozyme expressing clones (clones 3 and 4) derived from the MEL cells to examine the effect of the $p16^{INK4a}$ reduction on cell proliferation. Exponentially growing MEL clones were seeded in microtiter plates and allowed to grow. At different time points cells were collected and the number of cells counted (Fig. 4). The two Rz 89-12 clones proliferated considerably faster than the Va control clones (minus ribozyme) reflected by shorten-

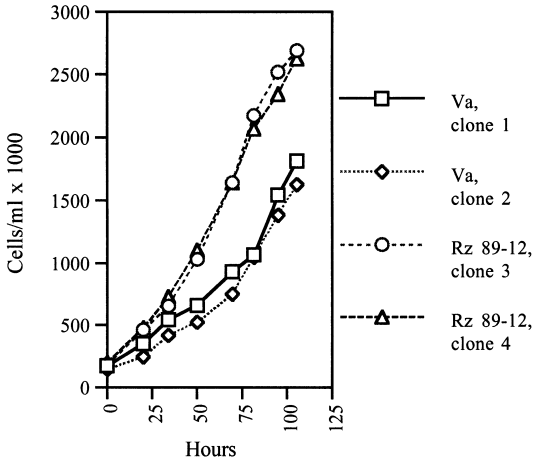


Fig. 4. Growth curves of the two Rz 89-12 clones and Va control clones. Cells were seeded ($1.5\times10^5$ cells per ml) in duplicates in 24-well dishes and two wells per clone were harvested and counted at different time points. The cell number represents mean values for each time point. The cell doubling time for each clone was determined on a logarithmic *y*-scale (not shown) from 0–75 h. Rz 89-12 clones, T2 = 23 h. Control Va clones, T2 = 30 h. The experiment presented here is a representative of three independent experiments.

ing of the doubling time to 23 h compared with the 30 h in control clones. These data suggest that the ribozyme-mediated reduction in $p16^{INK4a}$ protein levels is associated with accelerated progression through the cell cycle.

## 4. Discussion

The ribozyme technology has recently attracted considerable attention as an emerging strategy to selectively inactivate or downmodulate expression of specific genes, in either transient or sustained manner, without affecting gene structure. Despite the wide spectrum of potential biomedical applications [24], ranging from in vitro studies elucidating the roles of diverse regulatory proteins, up to gene therapy of human diseases, the widespread use of the ribozymes has been rather slow due, at least in part, to technical difficulties with their design (see also Section 1). The successful construction of the effective $p16^{INK4a}$-specific ribozyme, reported in our present study, therefore merits attention from both the point of view of the technology involved, as well as the potential biological applications of this new tool.

In terms of the technical aspects, our data support the notion that one of the critical parameters in the design of an efficient ribozyme is the identification of accessible single-stranded cleavage sites within the target RNA [14,15,24]. The choice of cleavage sites exclusively on the basis of sequence information often leads to disappointing failures. Here we have used computer modelling to predict the secondary structure of the $p16^{INK4a}$ mRNA, and based on the predicted minimum energy folding structure, the cleavage site at nucleotide 89 was chosen as a candidate target. This GUC site was predicted to be located in an accessible RNA loop structure according to the obtained computer model, and our results showed that the $p16^{INK4a}$-specific ribozymes indeed efficiently cleaved the mRNA after nt 89 at the expected site in vitro. In addition, the ribozymes reduced the level of translated $p16^{INK4a}$ by more than 95% when examined in the transcription/translation system, though this pronounced effect likely reflects the sum of the mRNA cleavage and contribution of antisense phenomena. Both the Rz 89-15 and Rz 89-12 cleaved with similar efficiency in the in vitro assays, suggesting that shortening of the target recognition sequence in the latter ribozyme did not significantly increase its catalytical activity.

To evaluate the ability of our new ribozyme to inactivate $p16^{INK4a}$ mRNA in vivo, we generated a series of cell clones upon stable transfection of the Rz 89-12 construct into murine erythroleukemia (MEL) cells. This cellular model was chosen based on the previously shown elevated expression of $p16^{INK4a}$ [23], and the demonstration that these cells harbor a functional RB pathway including the pRB tumor suppressor itself, and its key upstream regulators cyclin D2, D3, and Cdk4 [21]. The observed expression of the ribozyme in the transfected cells was driven both by the CMV promoter in the vector sequence, and from the intragenic polymerase III promoter within the Va I gene as determined by Northern blotting (our unpublished data). The significant effect of the ribozyme in live cells was reflected by considerably reduced expression of $p16^{INK4a}$, resulting in more than 70% decrease at the protein level. The ribozyme-mediated cleavage after nt 89 did not destabilize the $p16^{INK4a}$ transcript significantly, as documented by Northern blotting. On the other hand, the cleavage generated a truncated transcript which is most likely not translated to a functional protein in vivo. Evidence for the cleavage could be found on the RNA blots (see Fig. 3A), in the form of a shorter, 757-nt cleavage product that migrated slightly faster compared with the uncleaved product.

As the $p16^{INK4a}$ Cdk inhibitor and tumor suppressor normally retards or even blocks cell cycle progression [25–27], a rather strong prediction for a biological effect of an efficient $p16^{INK4a}$-specific ribozyme was that the ribozyme expressing cells may progress through the cell cycle with accelerated speed. This prediction was confirmed by the comparative growth curve experiments, in that the doubling time of the clones stably expressing the Rz 89-12 ribozyme was shortened by approximately 7 h relative to clones transfected with the vector DNA only. This result is consistent with the current stoichiometric models of action of the Cdk inhibitors through their physical interaction and/or disruption of the cyclin-Cdk complexes [1,5,6]. Since the degree of the biological effects of Cdk inhibitors including $p16^{INK4a}$ depends on their threshold level [1,5,6,27] significant biological effects can be expected not only following complete elimination, but also under conditions of significant reduction of the protein. The fact that the residual 25–30% of the $p16^{INK4a}$ protein are unable to preserve the normal duration of the cell cycle, leading to the observed acceleration of proliferation in our model, is reminiscent of naturally occurring tumor-associated point mutations of the $p16^{INK4a}$ gene resulting in protein products partly impaired in their function [27]. In view of the fact that such partially defective mutations have been selected for during the course of oncogenesis in vivo, the data presented here suggest that the expression of our new ribozyme can result in biologically meaningful effects. This conclusion is further substantiated by the fact that the level of $p16^{INK4a}$ expression in the majority of cell types, including the primary fibroblasts or epithelial cells, is below the level seen in the MEL cell line, possibly allowing for even more substantial reduction of $p16^{INK4a}$ levels by our ribozyme if applied in such models.

Finally, the high degree of specificity achieved by the ribozyme cleavage, further documented here by its strict selectivity

towards the murine transcript when compared with the human $p16^{INK4a}$ homologue, suggests its potential application in the difficult task to distinguish between the effects caused by the two alternative transcripts encoded by the INK4a locus [9–11] (see Section 1). The localization of the ribozyme cleavage site in exon E1α, and thus outside the sequence that overlaps with that encoding the $p19^{ARF}$ cell cycle inhibitor [9–11], indicates that the Rz 89-12 ribozyme could help clarify the present uncertainty about the role of the mouse $p16^{INK4a}$ as tumor suppressor. This highly debated issue was raised following demonstration that the tumor-prone phenotype originally observed in mice homozygously deleted for the exon 2 [28] encoding both the $p16^{INK4a}$ and $p19^{ARF}$ [10] can be largely recapitulated in gene knock-out animals specifically deprived of the $p19^{ARF}$ alone [29], thereby leaving the contribution of $p16^{INK4a}$ to the phenotype, and to mouse oncogenesis in general, subject to speculation. This conceptually important issue however represents only one of numerous potential applications of specific and efficient ribozymes against $p16^{INK4a}$, and it is our hope that this new tool will contribute to elucidation of the involvement of $p16^{INK4a}$ in regulation of fundamental biological processes including cell proliferation, replicative senescence, and multistep tumorigenesis.

*Acknowledgements:* This work was supported by grants from the Danish Cancer Society, and the Danish Medical Research Council (Grant no. 9600821).

## References

[1] Pines, J. (1996) Curr. Biol. 6, 1399–1402.
[2] Sherr, C.J. (1996) Science 274, 1672–1677.
[3] Bartek, J., Bartkova, J. and Lukas, J. (1996) Curr. Opin. Cell. Biol. 8, 805–814.
[4] Weinberg, R.A. (1995) Cell 81, 323–330.
[5] Harper, J.W. and Elledge, S.J. (1996) Curr. Opin. Genet. Dev. 6, 56–64.
[6] Sherr, C.J. and Roberts, J.M. (1995) Genes Dev. 9, 1149–1163.
[7] Hall, M. and Peters, G. (1996) Adv. Cancer Res. 68, 67–108.
[8] Kamb, A. (1995) TIG 11, 136–140.
[9] Stone, S., Jiang, P., Dayananth, P., Tavtigian, S.V., Katcher, H., Parry, D., Peters, G. and Kamb, A. (1995) Cancer Res. 55, 2988–2994.
[10] Quelle, D.E., Zindy, F., Ashmun, R.A. and Sherr, C.J. (1995) Cell 83, 993–1000.
[11] Duro, D., Bernard, O., Della, V.V., Berger, R. and Larsen, C.J. (1995) Oncogene 11, 21–29.
[12] Hasseloff, J. and Gerlach, W.L. (1988) Nature 334, 585–591.
[13] Bratty, J., Chartrand, P., Ferbeyre, G. and Cedergren, R. (1993) Biochim. Biophys. Acta 1216, 345–359.
[14] Lieber, A. and Strauss, M. (1995) Mol. Cell. Biol. 15, 540–551.
[15] Branch, A.D. and Klotman, P.E. (1998) Exp. Nephrol. 6, 78–83.
[16] Thompson, J.D., Ayers, D.F., Malmstrom, T.A., McKenzie, T.L., Ganousis, L., Chowrira, B.M., Couture, L. and Stinchcomb, D.T. (1995) Nucleic Acids Res. 23, 2259–2268.
[17] Lieber, A., He, C.Y., Polyak, S.J., Gretch, D.R., Barr, D. and Kay, M.A. (1996) J. Virol. 70, 8782–8791.
[18] Ventura, M., Wang, P., Ragot, T., Perricaudet, M. and Saragosti, S. (1993) Nucleic Acids Res. 21, 3249–3255.
[19] Priesli, S., Buonomo, S.B.C., Michienzi, A. and Bozzoni, I. (1998) RNA 3, 677–687.
[20] Superti-Furga, G., Bergers, G., Picard, D. and Bussilinger, M. (1991) Proc. Natl. Acad. Sci. USA 88, 5114–5118.
[21] Kiyokawa, H., Richon, V.M., Rifkind, R.A. and Marks, P.A. (1994) Mol. Cell. Biol. 14, 7195–7203.
[22] MacDonald, R.J., Swift, G.H., Przybyla, A.E. and Chirgwin, J.M. (1987) Methods Enzymol. 152, 219–227.
[23] Quelle, D.E., Ashmun, R.A., Hannon, G.J., Rehberger, P.A., Trono, D., Richter, K.H., Walker, C., Beach, D., Sherr, C.J. and Serrano, M. (1995) Oncogene 11, 635–645.
[24] Strauss, M. (1997) in: C. Lichtenstein and W. Nellen (Eds.), Antisense Technology: A Pratical Approach, pp. 221–239.
[25] Serrano, M., Hannon, G.J. and Beach, D. (1993) Nature 366, 704–707.
[26] Lukas, J., Parry, D., Aagaard, L., Mann, D.J., Bartkova, J., Strauss, M., Peters, G. and Bartek, J. (1995) Nature 375, 503–506.
[27] Koh, J., Enders, G.H., Dynlacht, B.D. and Harlow, E. (1995) Nature 375, 506–510.
[28] Serrano, M., Lee, H., Chin, L., Cordon-Cardo, C., Beach, D. and DePinho, R.H. (1996) Cell 85, 27–37.
[29] Kamijo, T., Zindy, F., Roussel, M.F., Quelle, D.E., Downing, J.R., Ashmun, R.A., Grosveld, G. and Sherr, C.J. (1997) Cell 91, 649–659.